Fundamental characterisation of sperrylite leaching behaviour in cyanide systems using XPS

Kathija Shaik[1], Hristo. Kolev[2], Zara. Cherkezova-Zheleva[2], and Jochen Petersen[1]

[1] *University of Cape Town, Institute of Catalysis*

[2] *Bulgarian Academy of Sciences*

Conventional matte-smelt-refine route

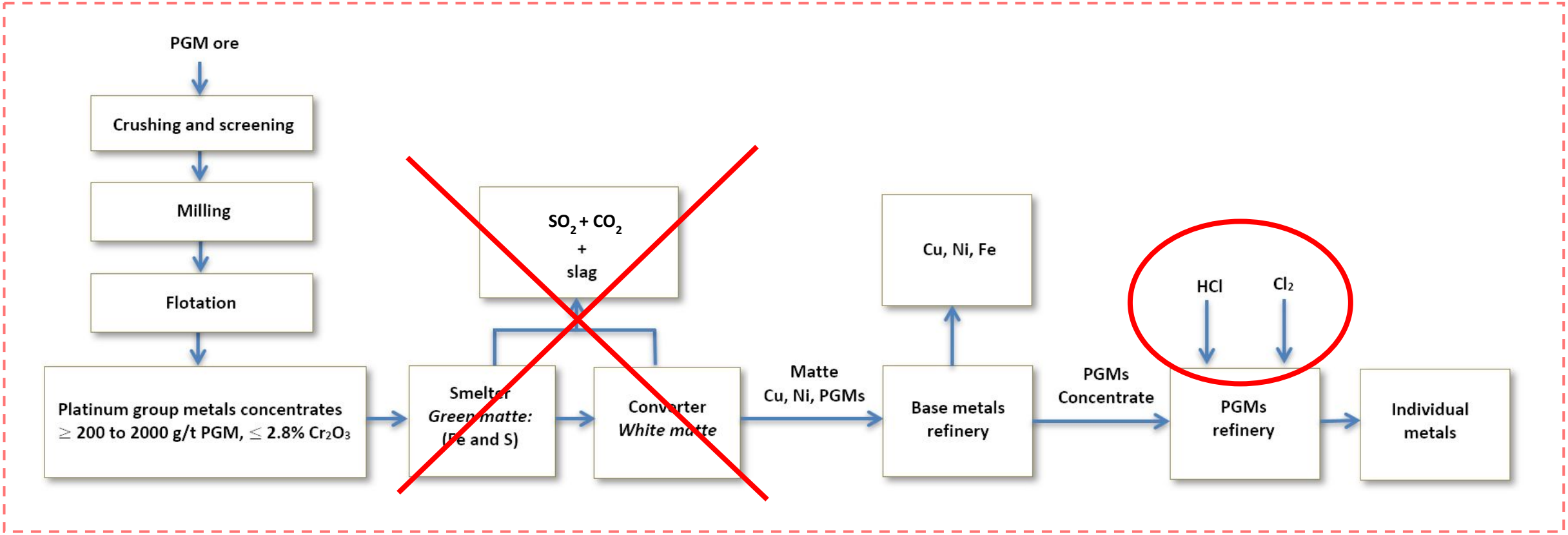

1. Mpinga, C. N. *et al.* (2015) 'Direct leach approaches to Platinum Group Metal (PGM) ores and concentrates: A review', *Minerals Engineering*, 78, pp. 93–113
2. Crundwell, F. K. *et al.* (2011) *Extractive Metallurgy of Nickel, Cobalt and Platinum-Group Metals*. Elsevier Ltd.

Pt leaching in cyanide systems

Sequential heap leach (Mwase et al. 2014)

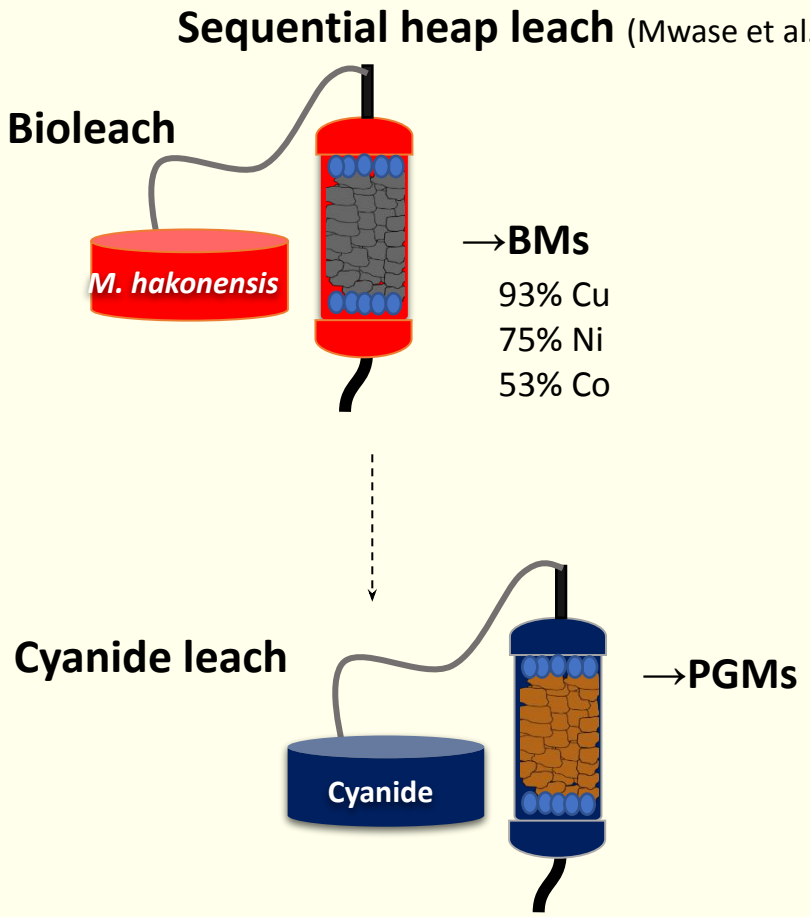

-25 mm +1 mm (C1)

- 6 mm +1 mm (C2)

Figure 1. Pt leach curves from cyanide experiments. Column 1: -25 +1 mm, Column 2: -6 +1 mm; both columns leached at 5 L/m2/hr with 5 g/L NaCN solution; 50°C; pH 10.4-10.7; aeration rate: 130 mL/min.

	Pt	Pd	Au
	%	%	%
Column 1	41.0	79.3	80.6
Column 2	55.9	100	88.4

1. Mwase, J., Petersen, J. and Eksteen, J. (2012a) 'Hydrometallurgy A conceptual fl owsheet for heap leaching of platinum group metals (PGMs) from a low-grade ore concentrate', *Hydrometallurgy*. Elsevier B.V., 111–112, pp. 129–135.
2. Mwase, J., Petersen, J. and Eksteen, J. (2012b) 'Hydrometallurgy Assessing a two-stage heap leaching process for Platreef fl otation concentrate', *Hydrometallurgy*. Elsevier B.V., 129–130, pp. 74–81.
3. Mwase, J., Petersen, J. and Eksteen, J. (2014) 'Hydrometallurgy A novel sequential heap leach process for treating crushed Platreef ore', *Hydrometallurgy*. Elsevier B.V., 141, pp. 97–104.

Sperrylite

Platinum arsenide mineral - $PtAs_2$

- Bushveld Igneous complex – South Africa
- Nickel deposits, Sudbury Basin – Canada
- Copper-nickel deposit, Eastern Siberia, Russia

$PtAs_2$

Most widespread platinum mineral and therefore economically important

The mineral is an opaque metallic tin white colour

Pyrite structure

Challenges

- Poor flotability
- Chemically stable
- Oxidation states of Pt and As are not well established

$PtAs_2$ in cyanide based systems

(Mwase & Petersen, 2017)

- Investigated the leaching behaviour of $PtAs_2$ in cyanide-ferricyanide systems
- Slow leach kinetics attributed to:
  - Refractory nature of $PtAs_2$
  - Formation of an As enriched inhibition layer
- Proposed that washing and contacting the mineral with fresh solution can eliminate the inhibition layer

Aim

- ***Evaluate the formation of As/Pt enriched precipitates and establish their chemical compositions, by the use of non-invasive surface analytical techniques.***

- ***Determine the oxidation states of platinum and arsenic and monitor how they evolve during leaching under varied system conditions.***

Experimental approach

Crystal | Coarse (0.5 mm – 3 mm) | Fine (< 5 µm)

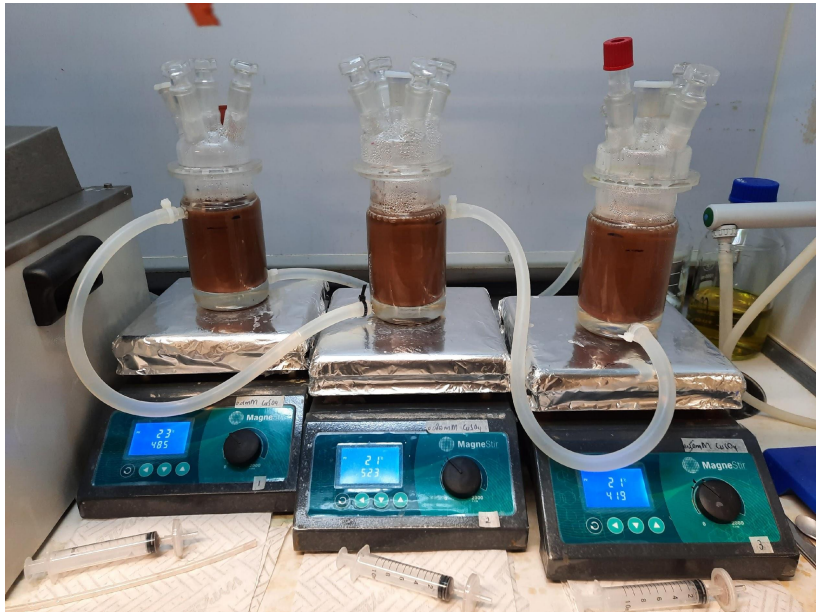

Figure 2. Experimental setup for the leaching process

- Sample originated from the nickel ore deposit of the Sudbury Basin in Ontario, Canada.
- XRD established that the sample was 100% $PtAs_2$
- SEM-EDS revealed that natural $PtAs_2$ comprised of 55.13% Pt and 44.87% As and showed a few impurities of Cu, Si, and S.

1. Base Case

- 100 mM NaCN
- 20 mM $K_3[Fe(CN)_6]$
- 45 °C, 500 rpm, 24 h duration
- 0.75 g finely ground $PtAs_2$ in 250 mL

2. Variables investigated

- **Lixiviant** – NaCN (100, 200 mM)
- **Oxidant** – $K_3[Fe(CN)_6]$ (20, 40 mM)
- **Catalyst** – $CuSO_4 \cdot 5H_2O$ (0.05 mM)
- **Temperature** – 45, 55 °C
- **Particle size** – crystalline, coarse, fine

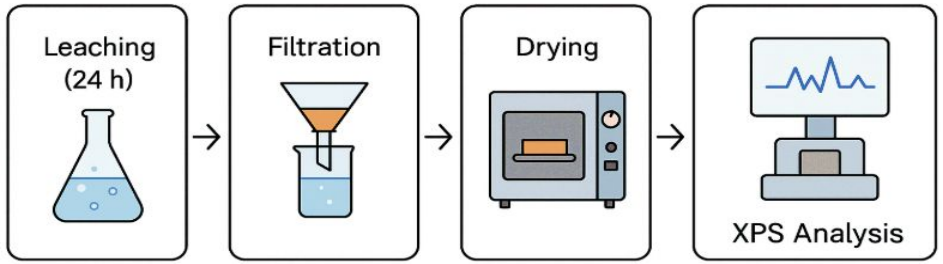

Figure 3. Sequential process showing sample preparation from leaching to XPS surface analysis.

Experimental approach

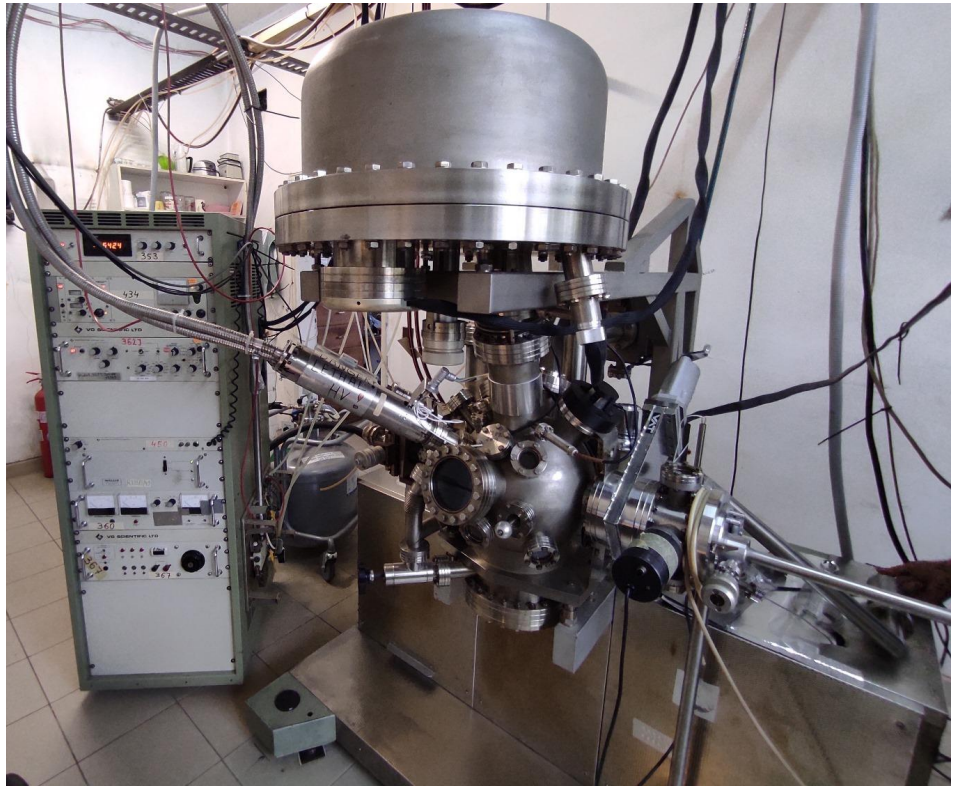

Figure 4. ESCALAB MkII electron spectrophotometer

1. Ex-situ XPS Analysis

- IC-BAS (Bulgaria)
- ESCALAB MkII electron spectrophotometer

2. Mechanism

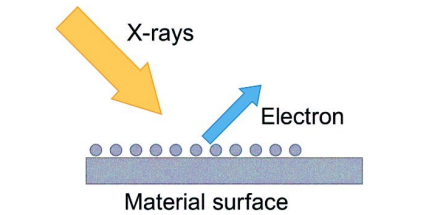

X-ray Photoelectron Spectroscopy (XPS) analyzes a material's surface by measuring the energies of electrons emitted when the surface is irradiated with X-rays, revealing its elemental composition and chemical states.

3. Operating conditions

- **Base pressure:** 5×10^{-10} mbar
- **X-ray source:** MgKα: 1253.6 eV

4. Data analysis

- **Data processing:** SpecsLab2 & Casa XPS software
- **Peak fitting:** Gaussian–Lorentzian symmetric functions

Untreated crystal & crushed sample

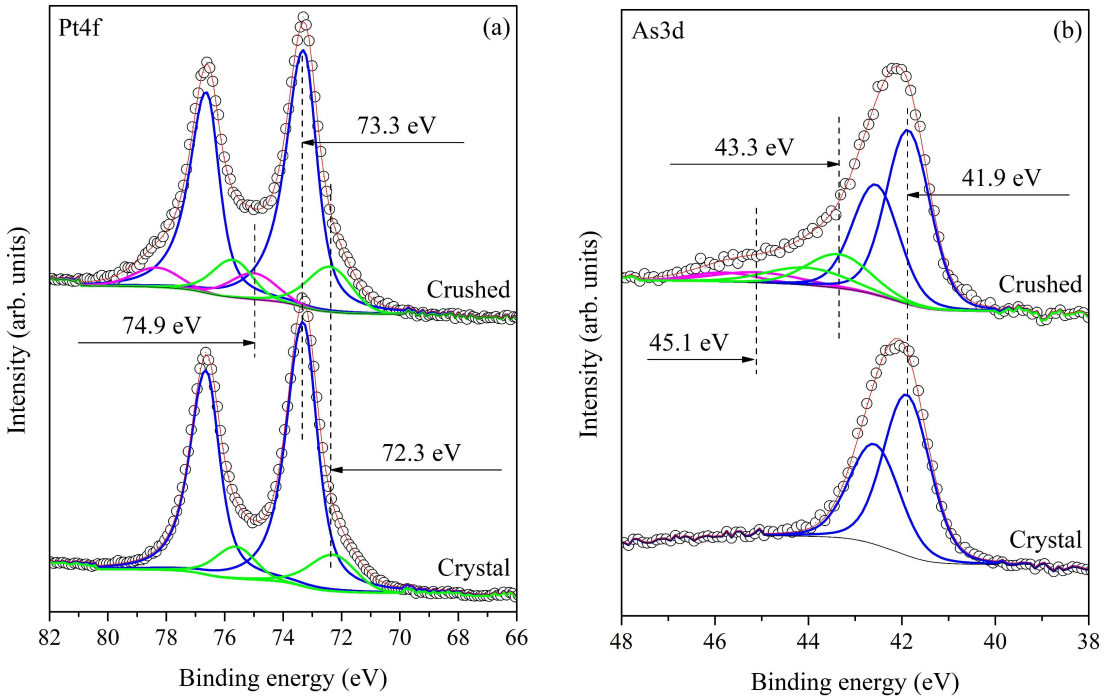

Figure 5. Pt4f and As3d XPS spectra of the untreated crystalline and crushed sperrylite sample

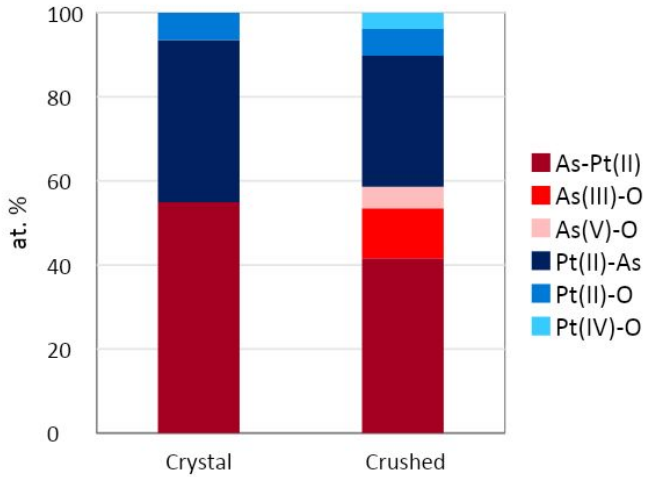

Figure 6. Relative distribution of Pt and As species determined by XPS analysis

Table 1. Relative proportions of the different Pt and As species determined by XPS analysis

Peak	Assignment	Binding Energy (eV)	Crystal (%)	Crushed (%)
Pt4f	Pt(II)-As	73.3	38.6	31.18
	Pt(II)-O	72.3	6.47	6.38
	Pt(IV)-O	74.9	-	3.85
As3d	As(-I)-Pt	41.9	54.93	41.58
	As(III)-O	43.3	-	11.88
	As(V)-O	45.1	-	5.13

Effect of various parameters

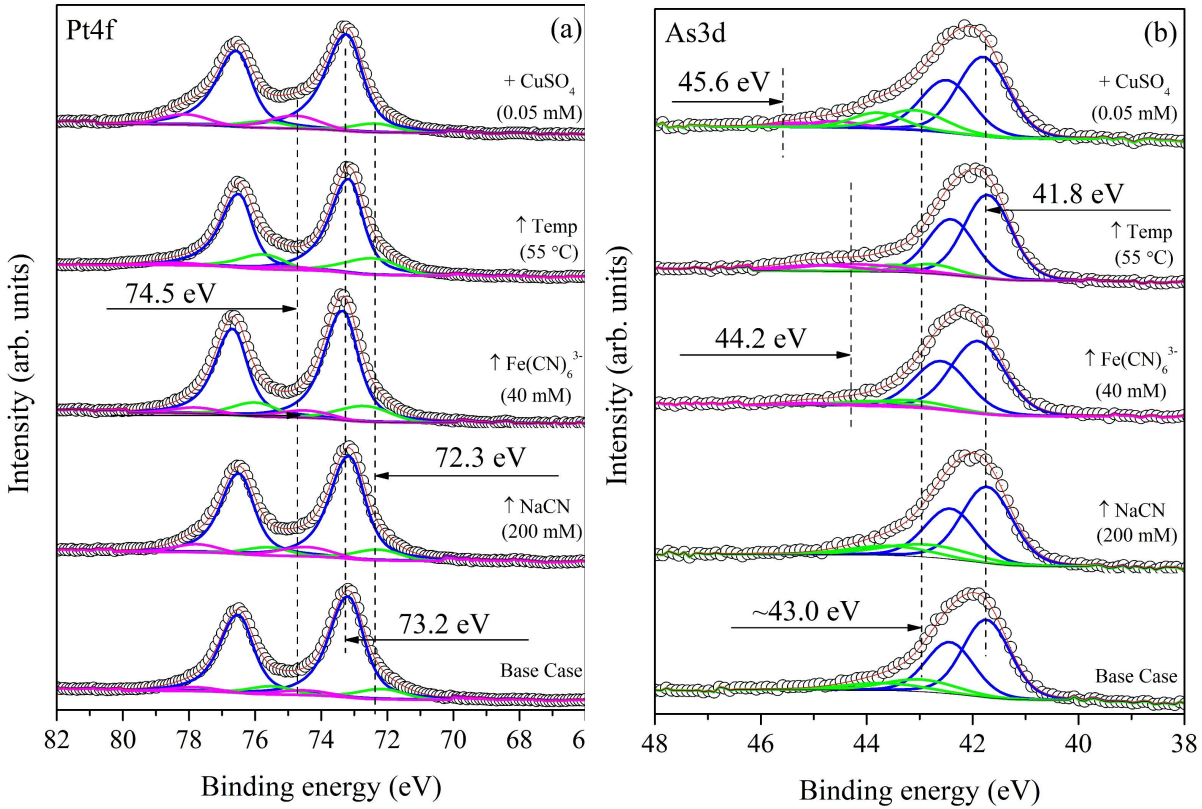

Figure 7. Pt4f and As3d XPS spectra of crushed sperrylite under varied leach conditions

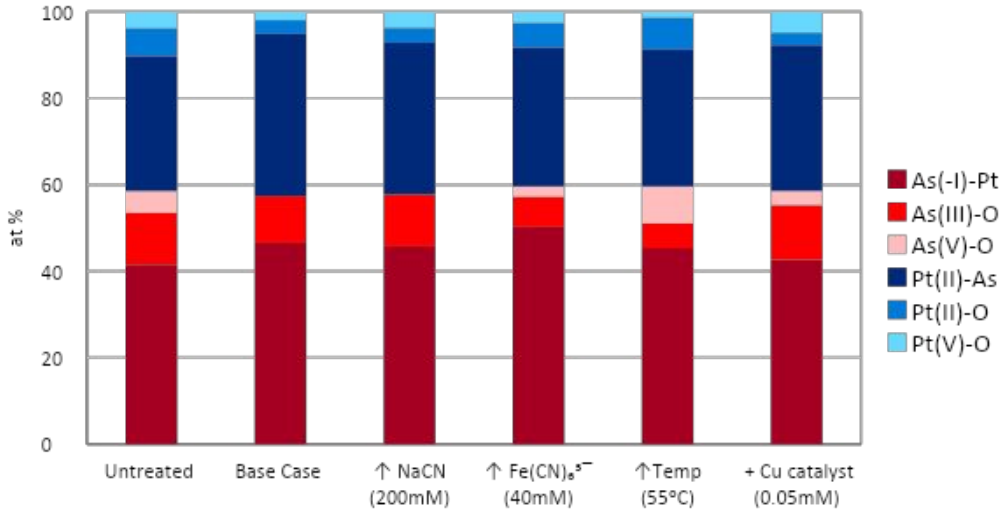

Figure 8. Relative distribution of Pt and As species determined by XPS analysis under varied conditions

Table 2. Relative proportions of the different Pt and As species determined by XPS analysis under varied conditions

Peak	Assignment	Binding Energy (eV)	Untreated	Base Case	↑ NaCN (200mM)	↑ $Fe(CN)_6^{3-}$ (40mM)	↑ Temp (55 °C)	+ Cu catalyst (0.05mM)
Pt4f	Pt(II)-As	73.2	31.18	37.47	35.03	32.11	31.68	33.61
	Pt(II)-O	72.3	6.38	3.14	3.46	5.64	7.36	2.87
	Pt(IV)-O	74.5	3.85	1.96	3.74	2.60	1.38	4.87
As3d	As(-I)-Pt	41.8	41.58	46.56	45.75	50.25	45.31	42.61
	As(III)-O	43.0	11.88	10.87	12.02	6.95	5.72	12.64
	As(V)-O	44.2	5.13	-	-	2.45	8.56	3.40

Effect of particle size

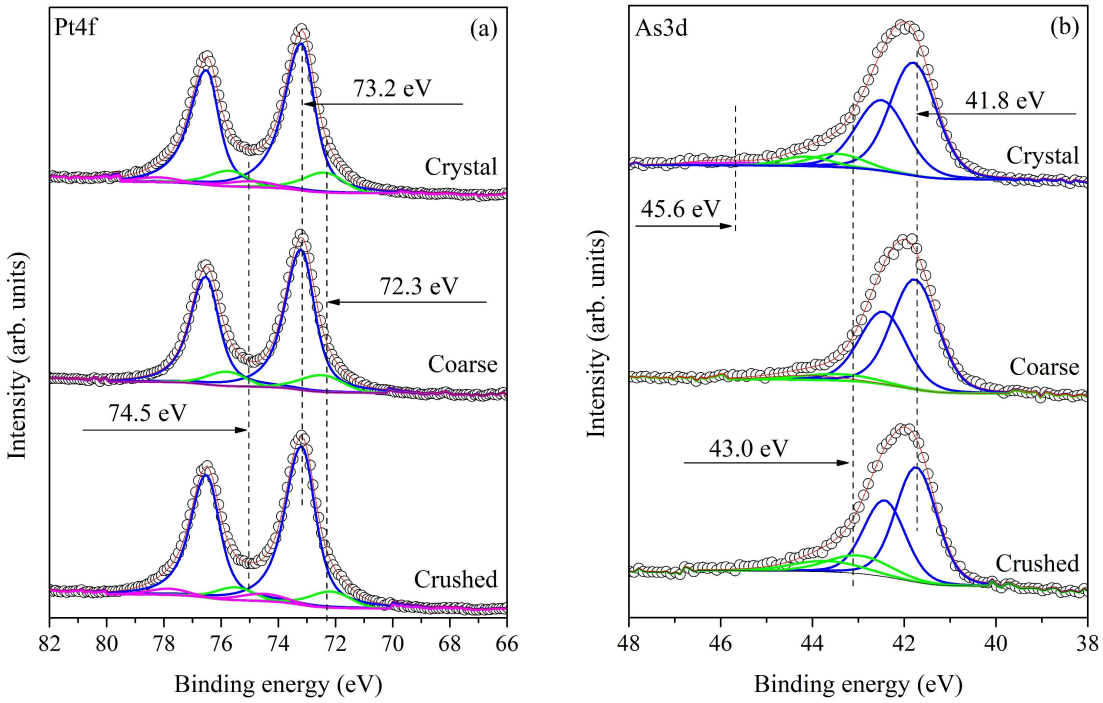

Figure 9. Pt4f and As3d XPS spectra of crushed, coarse, and crystalline leached samples

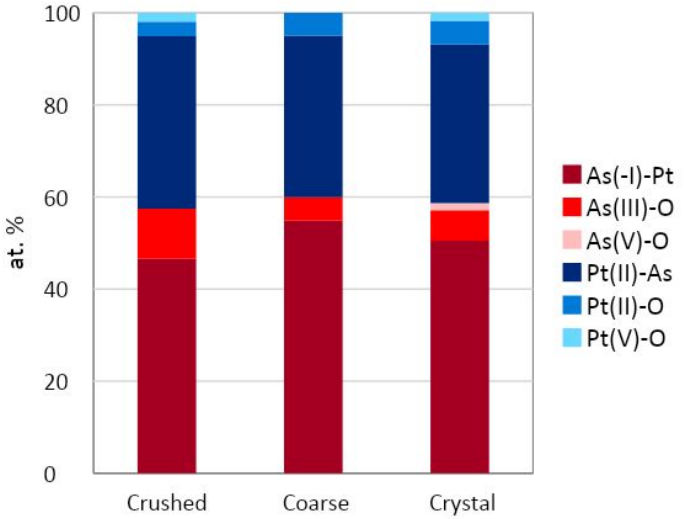

Figure 10. Relative distribution of Pt and As species determined by XPS analysis at varied particle size

Table 3. Relative proportions of the different Pt and As species determined by XPS analysis

Peak	Assignment	Binding energy (eV)	Crushed (%)	Coarse (%)	Crystal (%)
Pt4f	Pt(II)-As	73.2	37.47	35.17	34.43
	Pt(II)-O	72.3	3.14	4.93	5.18
	Pt(IV)-O	74.5	1.96	-	1.75
As3d	As(-I)-Pt	41.8	46.56	54.84	50.52
	As(III)-O	43.0	10.87	5.06	6.61
	As(V)-O	45.6	-	-	1.51

Effect of re-leach

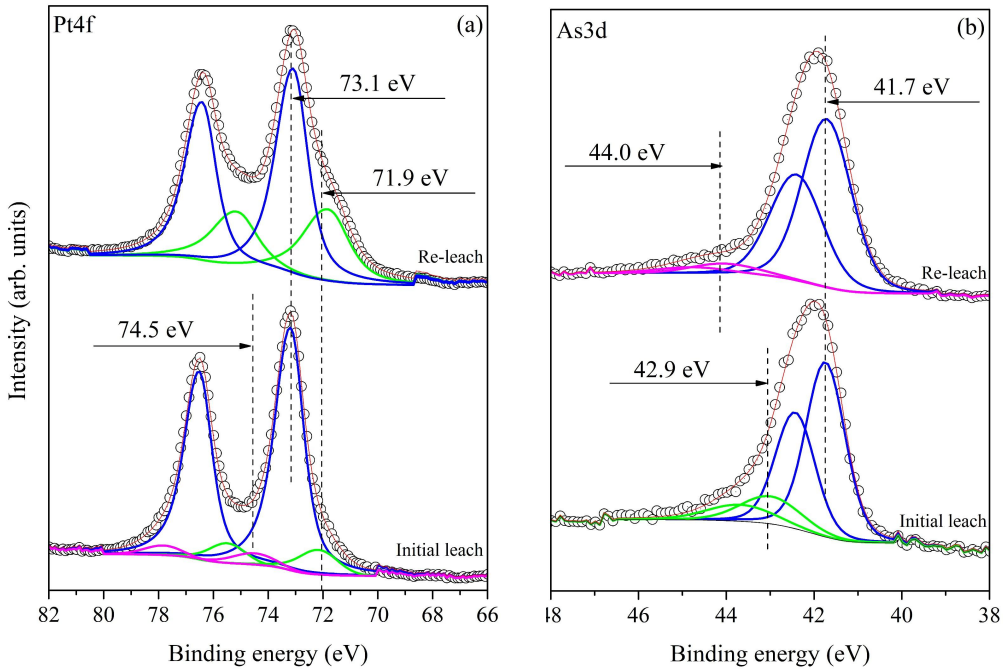

Figure 11. Pt4f and As3d XPS spectra after initial and re-leach step

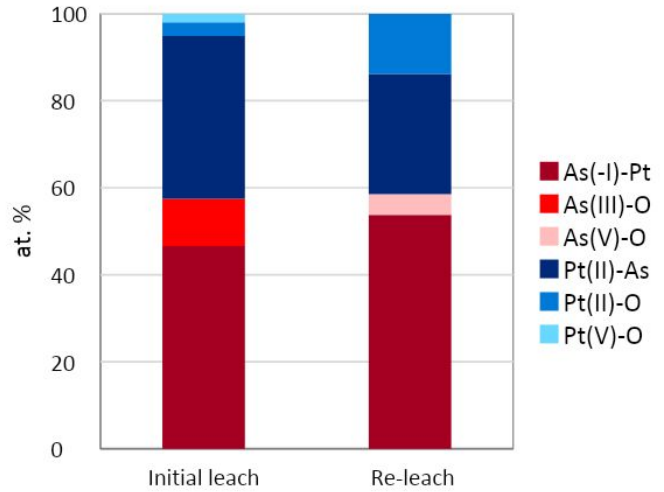

Figure 12. Relative distribution of Pt and As species determined by XPS analysis after initial and re-leach step

- During the re-leach step, the process exposed the underlying bulk state

Table 4. Relative proportions of the different Pt and As species determined by XPS analysis

Peak	Assignment	Binding energy (eV)	Initial leach (%)	Re-leach (%)
Pt4f	Pt(II)-As	73.1	37.47	27.63
	Pt(II)-O	71.9	3.14	13.82
	Pt(IV)-O	74.5	1.96	-
As3d	As(-I)-Pt	41.7	46.56	53.78
	As(III)-O	42.9	10.87	-
	As(V)-O	44.0	-	4.76

Key findings

- XPS analysis revealed the key surface species present on sperrylite.
  Bulk unoxidised sperrylite lattice Pt(II)–As (≈73 eV) and As(–I)–Pt (≈41.8 eV)
  Surface oxidation products Pt(II)–O (≈72 eV), Pt(IV)–O (≈74.5 eV), As(III)–O (≈43 eV) and As(V)–O (44.5 eV)

- After 24 hours, leaching largely removed surface oxides from the crushed sample, exposing the underlying bulk Pt(II)–As and As(–I)–Pt species without generating an additional oxide layer.

- The coarse sample was dominated by partially oxidised species (Pt(II)–O and As(III)–O), indicating a stable surface environment favoring lower oxidation states.

- The crystalline sample, initially low in oxides, produced higher proportions of fully oxidised species (Pt(IV), As(III), As(V)) after leaching, reflecting greater surface reactivity.

- The re-leach effectively removed As(III)-O and Pt(IV)-O; however, the surface remained highly enriched in Pt(II)-O, suggesting incomplete removal of the oxide layer.

Acknowledgements

Thank you

Thank you

Thermodynamic analysis

Complete reactions	ΔG^0 (kJ/mol)
$Pt + 4CN^- + 2Fe(CN)_6^{3-} \rightleftharpoons Pt(CN)_4^{2-} + 2Fe(CN)_6^{4-}$	-6.15
$PtAs_2 + 4CN^- + 6OH^- + 8Fe(CN)_6^{3-} \rightleftharpoons Pt(CN)_4^{2-} + 2H_3AsO_3 + 8Fe(CN)_6^{4-}$	-395.46
$PtAs_2 + 4CN^- + 8OH^- + 8Fe(CN)_6^{3-} \rightleftharpoons Pt(CN)_4^{2-} + 2AsO_2^- + 4H_2O + 8Fe(CN)_6^{4-}$	-450.58
$PtAs_2 + 4CN^- + 8OH^- + 8Fe(CN)_6^{3-} \rightleftharpoons Pt(CN)_4^{2-} + 2H_2AsO_3^- + 2H_2O + 8Fe(CN)_6^{4-}$	-451.30
$PtAs_2 + 4CN^- + 10OH^- + 8Fe(CN)_6^{3-} \rightleftharpoons Pt(CN)_4^{2-} + 2HAsO_3^{2-} + 4H_2O + 8Fe(CN)_6^{4-}$	-483.92
$PtAs_2 + 4CN^- + 12OH^- + 8Fe(CN)_6^{3-} \rightleftharpoons Pt(CN)_4^{2-} + 2AsO_3^{3-} + 4H_2O + 8Fe(CN)_6^{4-}$	-489.54
$PtAs_2 + 4CN^- + 14OH^- + 12Fe(CN)_6^{3-} \rightleftharpoons Pt(CN)_4^{2-} + 2HAsO_4^{2-} + 6H_2O + 12Fe(CN)_6^{4-}$	-847.60
$PtAs_2 + 4CN^- + 16OH^- + 12Fe(CN)_6^{3-} \rightleftharpoons Pt(CN)_4^{2-} + 2AsO_4^{3-} + 8H_2O + 12Fe(CN)_6^{4-}$	-870.74

- Oxidation of $PtAs_2$ by $Fe(CN)_6^{3-}$ produces negative G^0 values → a spontaneous reaction that is thermodynamically favourable
- As species with higher oxidation states correlates to higher negative G^0 values, and this can be seen for As(V)
- Oxidation of sperrylite occurs more easily than metallic platinum by comparison of the G^0 values.